Nanocrystalline TiO 2 /ZnO Thin Films: Fabrication and Application to Dye-Sensitized Solar Cells

ARTICLE *in* THE JOURNAL OF PHYSICAL CHEMISTRY B · JANUARY 2006

Impact Factor: 3.3 · DOI: 10.1021/jp0531560 · Source: PubMed

THE JOURNAL OF PHYSICAL CHEMISTRY B

Article

Nanocrystalline TiO/ZnO Thin Films: Fabrication and Application to Dye-Sensitized Solar Cells

Rajaram S. Mane, Won Joo Lee, Habib M. Pathan, and Sung-Hwan Han

J. Phys. Chem. B, **2005**, 109 (51), 24254-24259 • DOI: 10.1021/jp0531560

Nanocrystalline TiO_2/ZnO Thin Films: Fabrication and Application to Dye-Sensitized Solar Cells

Rajaram S. Mane, Won Joo Lee, Habib M. Pathan, and Sung-Hwan Han*

Inorganic Nano-Materials Laboratory, Department of Chemistry, Hanyang University, Sungdong-Ku, Haengdang 17, Seoul 133-791, Republic of Korea

Received: June 12, 2005; In Final Form: October 25, 2005

Nanocrystalline TiO_2 thin films composed of densely packed grains were deposited onto indium-doped tin oxide (ITO)-coated glass substrates at room temperature using a chemical bath deposition technique. A layer-by-layer (LbL) process was utilized to obtain a 1.418-μm-thick TiO_2/ZnO structure. The TiO_2 surface was super-hydrophilic, but its hydrophilicity decreased considerably after ZnO deposition. Other TiO_2/ZnO films were studied to assess their suitability as photoelectrodes in dye-sensitized solar cells (DSSCs).

Introduction

TiO_2 is one of the most extensively studied oxides because of its remarkable optical and electronic properties. Because of strong confinement, the electrical and optical properties of nanocrystalline TiO_2 thin films vary significantly with grain size, and this ability to tune their physical properties makes them an important candidate for potential application as photoelectronic materials.[1,2] The electron flow through semiconducting TiO_2 thin films occurs via a hopping mechanism, which exhibits a slow nonexponential current and charge recombination, thus limiting efficient charge transfer.[3,4]

ZnO is also an important semiconductor and has been investigated widely for its catalytic, electrical, optical, and photochemical properties[5−8] and for application in blue/ultraviolet (UV) optoelectronic devices and in piezoelectric devices. For example, Huang and co-workers[9] observed a UV laser emission at room temperature in ZnO nanowires. Because of the interesting effects of size and quantum confinement, much effort has been devoted to growing ZnO whiskers, nanowires, and nanobelts over the past decade.[10,11]

Dye-sensitized metal oxides have also been extensively investigated. Gratzel's group has successfully developed a high power conversion efficiency of about 10% for thick spin-coated nanoporous TiO_2 films for use as a photoelectrode.[12] Other metal oxides, for example, MgO, CdO, Fe_2O_3, SnO_2, and ZnO have been tested for dye-sensitizing properties. Out of these, ZnO has received much attention owing to its band gap energy (3.4 eV), which is similar to TiO_2 (3.2 eV). Other semiconductors showing a lower power conversion efficiency than TiO_2 have exhibited similar values when used as composite films, including ZnO/SnO_2,[13] CdS/MgO,[14] and SnO_2/MgO.[15] Recently, dye-sensitized ZnS/ZnO composite thin films with a hole-injecting poly(ethylenedioxythiophene)/polystyrensulfonic acid (PEDOT:PSS) layer have been successfully developed by Liao and Ho[16] and have a reported conversion efficiency of 0.08−0.82%, depending on the preparation conditions.

To solve the problem of slow charge flow, we proposed using a ZnO conical surface morphology grown vertically from an electrode to replace existing mesoporous electrodes using a layer-by-layer (LbL) process onto chemically deposited compact and densely packed nanocrystalline TiO_2 thin films. The use of nanocrystalline TiO_2 films permits the formation of an energy barrier at the electrode/electrolyte interface, thus reducing the recombination rate and improving the cell performance. The ZnO conical morphology has a large surface area and long conduction pathways that lead straight to the electrode for efficient and fast charge transport, along with a higher dye storage capacity. A photosensitive dye was adsorbed into the ZnO cones to absorb light and create excited electrons and a transparent nanocrystalline TiO_2 and indium-doped tin oxide (ITO) encapsulated the cell, which was then filled with active electrolyte to achieve active hole conduction. The nanocrystalline TiO_2/ZnO electrodes were examined using X-ray diffraction, optical absorption, and water contact angle techniques. The surface morphology of the TiO_2 and TiO_2/ZnO films were observed using high-resolution scanning electron microscopy. The dye adsorption in the ZnO conical structure electrode was confirmed from photoimages taken with a Sony digital camera using a white background. Finally, the performance and durability of the dye-sensitized TiO_2/ZnO electrodes were studied in different electrolytes from the I−V curve data and stability tests, respectively.

Experimental Details

To obtain nanocrystalline TiO_2/ZnO, the following procedure was used. Liquid $TiCl_3$ was dissolved in water in the desired concentration. Two milliliters of $TiCl_3$ (20−30 wt % in HCl, Aldrich Chemicals, U.S.A.) was added to an ice-cooled mixture consisting of 20 mL of deionized water (18 MΩ cm). The pH was adjusted to 3.0−3.5 using a 7% ammonium hydroxide solution with constant stirring. After stirring for 30 min, a homogeneous violet-black colored solution was obtained, which was stable for a period of several hours at room temperature. Clean indium tin oxide (ITO) substrates were floated on the surface of the dilute solution at room temperature (27 °C) to deposit a thin film. The solution became turbid after soaking for a period of about 15 min. After soaking for 6 h, the substrate was carefully rinsed with deionized water, ultrasonically cleaned with deionized water, and then dried under flowing argon gas. After a period of 6 h, the solution color changed from violet-

* To whom correspondence should be addressed. Tel.: + 822 2292 5212. Fax: +822 2299 0762. E-mail: shhan@hanyang.ac.kr.

10.1021/jp0531560 CCC: $30.25
Published on Web 12/06/2005

black to off-white, and further dipping of the ITO substrate into the solution resulted in dissolution of both the TiO_2 and the ITO.

The ITO/TiO_2 film was immersed in 0.1 M $ZnCl_2$ complexed with ammonium hydroxide and hydrogen peroxide for a period of 25 s. Excess ammonium hydroxide solution was used to control the pH of the $ZnCl_2$ solution to ~14. Addition of the ammonium hydroxide solution to the $ZnCl_2$ resulted in the formation of a $Zn(OH)_2$ precipitate, but this redissolved in excess ammonium hydroxide to form the tetra-amine zinc complex. Then, the substrate was immersed in distilled water at 90 °C. High temperatures promoted the adherence of the ZnO film. In the first preparative stage, the ammonia−zinc ions complex was adsorbed onto the substrate surface, and in the second preparative stage, the hydroxide of the anion precursor solution was adsorbed onto the surface and reacted with the adsorbed zinc species to yield zinc hydroxide, which in turn was converted into ZnO. There were several insoluble zinc species present in a reaction bath containing OH^-, NH_3, and Zn^{2+} ions. The Zn was present as soluble Zn^{2+} ions for pH < 7.5, as ZnO^{2-} ions for pH > 13.7, and as insoluble $Zn(OH)_2$ for 7.5 < pH < 13.7.

The nanocrystalline TiO_2/ZnO film electrodes were examined with a Philips Japan MPD 1880 X-ray powder diffractometer using Cu Kα radiation ($V = 40$ keV and $I = 100$ mA), along with scanning electron microscopy (SEM) JEOL, with an energy-dispersive X-ray analysis (EDX) attachment and water contact angle measurements using a Surface Electo-Optics, Korea Model-Phoenix 150, contact angle analyzer. UV−vis spectra were recorded using a Cary Japan Model 100 CONC spectrophotometer. The TiO_2 and TiO_2/ZnO films were coated with a 100-nm-thick platinum layer using a Polaron SEM sputter coating unit (model E-2500) before obtaining the SEM images. The dye-immobilized TiO_2/ZnO electrode and the 100-nm-thick Pt-sputtered ITO were sandwiched together using a cell holder, into which an electrolyte solution was infiltrated using a fine 10 mL nontoxic Kovax syringe. Ruthenium(II) *cis*-di(thiocyano)bis(2,2′-bypyridyl-4,4′-dicarboxylic acid) (N3) dye was adsorbed into the TiO_2/ZnO surface by refluxing the electrode in dilute ethanol at 45 °C for 48 h. To obtain the ionic electrolyte (modified) solution, 15 mL of methoxyacetonitrile (98%) was placed in a beaker containing 0.6 M 1-hexyl-2-3-dimethylimidazolium iodide (C6DMI), 0.1 M lithium iodide (LiI), 0.05 M iodide (I_2), and 0.5 M 4-*tert*-butylpyridine (*t*-BPy), and the mixture was stirred for 30 min and stored in the dark for further use. Photoelectrochemical cell (PEC) measurements were performed using a 1-kW xenon lamp with a photointensity of 80 mW/cm^2. The dye-sensitized TiO_2/ZnO photoelectrode of the cell had an effective electrode area of 0.28 cm^2. In the stability tests, the same instrument using a different operational program (i.e., short circuit current vs time function) was used.

Results and Discussion

Figure 1 shows photoimages of TiO_2, TiO_2/ZnO, and TiO_2/ZnO with N3 dye, respectively. The violet-colored TiO_2 thin film can be clearly seen. It is known that titanium in aqueous solution can form a series of colored peroxotitanium complexes, depending on the pH of the solution.[17] At low pH, the ratio of peroxo(O−O) groups to titanium in the species is 1:1, although the exact nature of the species in the acid solutions remains controversial.[18] In our experiments, as the pH of the deposition solution was 3.0, hydrolyzed titanium cations formed a hydrous oxide precipitate by condensing via the olation and oxolation reactions.[19] In the literature, formation of the violet color due to interference is suggested by Zumeta et al.[20] After ZnO film deposition, the color changed to white (Figure 1b), and after

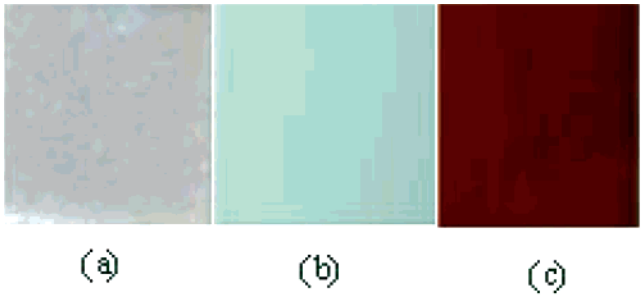

Figure 1. Photoimages of the surfaces of (a) TiO_2, (b) TiO_2/ZnO, and (c) TiO_2/ZnO with N3 dye. The images were taken under a white light source.

dye adsorption, the TiO_2/ZnO film surface became red, as seen in Figure 1c, confirming dye adsorption had taken place.

X-ray diffraction was used to confirm the formation of ZnO on the ITO/TiO_2 substrates and the crystallinity of the TiO_2 coating. No difference was observed between the XRD patterns corresponding to the ITO-coated glass and the as-deposited TiO_2 film on the ITO-coated glass substrate (not shown), which indicates a very low degree of crystallinity and the nanoparticle character of the film.[21] After ZnO deposition (see Figure 2a), diffraction peaks at $2\theta = 34.42$, 36.25, 47.54, 62.87, and 68° were observed, which correspond to the (002), (101), (102), (103), and (112) reflections of zinc oxide, respectively. The peaks were very sharp, implying the size of the ZnO cones was large. Here, we present only the experimental results from samples with 25 deposition cycles. The EDAX spectra of the TiO_2/ZnO samples are shown in Figure 2b. The presence of Si, In, and Ti corresponds to the ITO and TiO_2 substrates on which the ZnO was deposited. The sputter-coated 100-nm thick platinum also exhibited a peak. An elemental analysis for zinc and oxygen was carried out, and the stoichiometric ratio of Zn/O in the ZnO was approximately 1:1. Figure 3 shows SEM observations of the surface morphology of the TiO_2 and TiO_2/ZnO thin films. The TiO_2 film (Figure 3a) was composed of closely packed spherical nanoparticles, about 30−40 nm in diameter. An accurate size measurement of the TiO_2 spherical grains was difficult to perform due to practical limitations of the SEM. After ZnO deposition (Figure 3b), irregular, randomly oriented cones were clearly observed. As can be seen from the SEM data, the ZnO surface morphology exhibited empty spaces between the cones.

A surface wettability test on metal chalcogenide and oxide surfaces is an effective and well-defined diagnostic tool to check their feasibility as suitable candidates for high solar energy devices and dye adsorption. The wetting of a solid with water, where air is the surrounding medium, is dependent on the relationship between the existing interfacial tensions (water/air, water/solid, and solid/air). The ratio between these tensions determines the contact angle, θ, between a water droplet on a given surface. If the wettability is high, then θ will be small and the surface is classed as hydrophilic. To form a superhydrophilic TiO_2 surface, Wang et al.[22] suggested the use of ammonium hexafluorotitanate. The mechanism of the conversion from a hydrophobic to a hydrophilic character under UV illumination was explained by assuming that surface Ti^{4+} sites were reduced to Ti^{3+} states via photogenerated electrons and oxygen vacancies were generated through the oxidation of bridging O^{2-} species to form oxygen via photogenerated holes. Sun et al.[23] proposed a detailed mechanism for the formation of a hydrophilic TiO_2 surface with a water contact angle of 54° by considering surface defective sites.

In our work, the use of a Ti^{3+} source suggests that the above mechanism does not occur. This was confirmed by irradiating

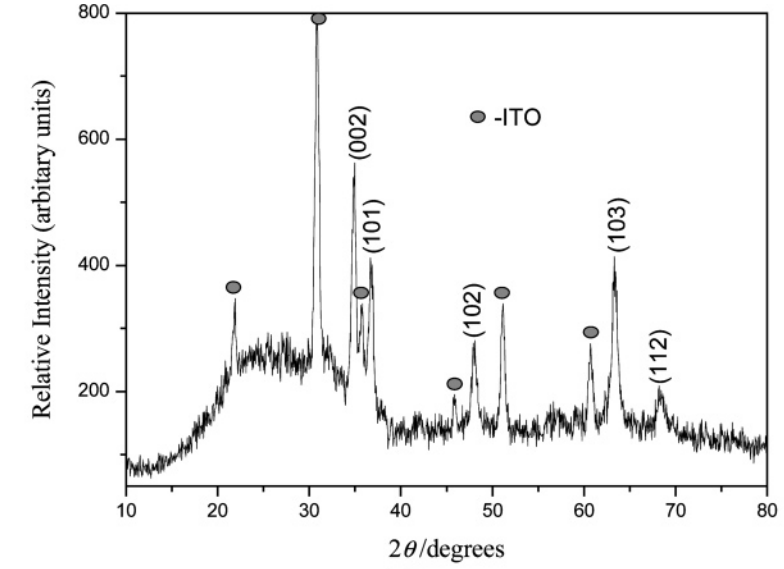

(a)

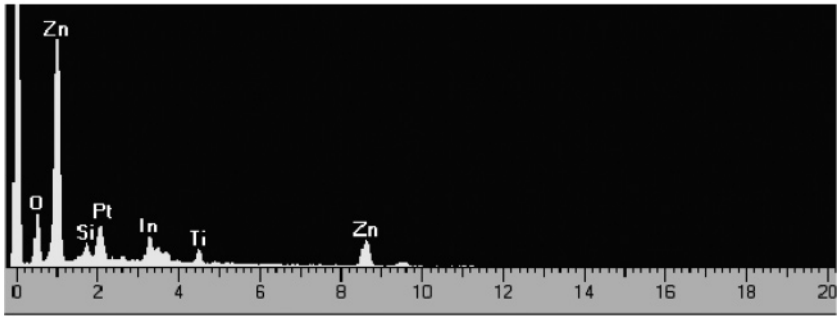

Elmt	Spect. Type	Apparent Conc.	Stat. Sigma	k Ratio	k Ratio Sigma
O K	ED	56.594	1.271	1.06279	0.02387
Zn K	ED	37.671	1.448	0.37671	0.01448

Elmt	Spect. Type	Inten. Corrn.	Std Corrn.	Element %	Sigma %	Atomic %
O K	ED	1.088	0.52	54.72	1.10	53.16
Zn K	ED	0.875	1.01	45.28	1.10	46.84
Total				100.00		100.00

(b)

Figure 2. (a) XRD profile of TiO_2/ZnO thin films, confirming the formation of ZnO on TiO_2 and (b) a typical EDAX spectra of TiO_2/ZnO on an ITO substrate taken while recording an SEM image. Analysis was carried out only for zinc and oxygen.

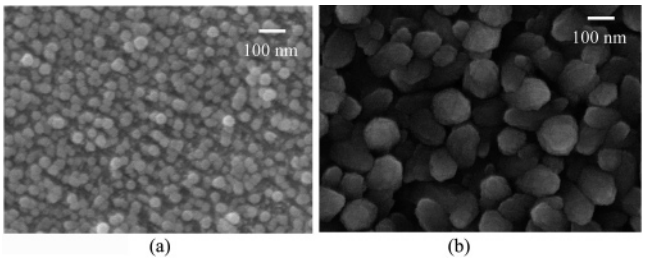

Figure 3. SEM images of (a) the as-deposited TiO_2 thin film and (b) with TiO_2/ZnO thin film deposition. The images were recorded at different magnification due to the differences between the structure of the TiO_2 and ZnO samples.

the TiO_2 surface with UV radiation and detecting no change in the water contact angle, even after a period of 12 h. These experimental results demonstrate that this solution is a good precursor for coating titanium oxide and that coatings treated

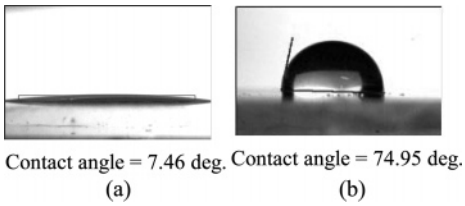

Figure 4. Surface wettability measurements vs water contact angle on (a) TiO_2 and (b) TiO_2/ZnO thin film surfaces.

at lower temperatures show good hydrophilic properties. The as-deposited TiO_2 nanocrystalline surface exhibited a super-hydrophilic surface (Figure 4a) because the water contact angle was $<20°$ (Figure 4a). The nanocrystalline compact TiO_2 surface may have a super-hydrophilic nature due to the direct relationship the surface tension has with the surface energy. Figure 4b shows that the TiO_2/ZnO film surface had an increased water contact angle of 74.95° (±1.5°). An increase in water contact

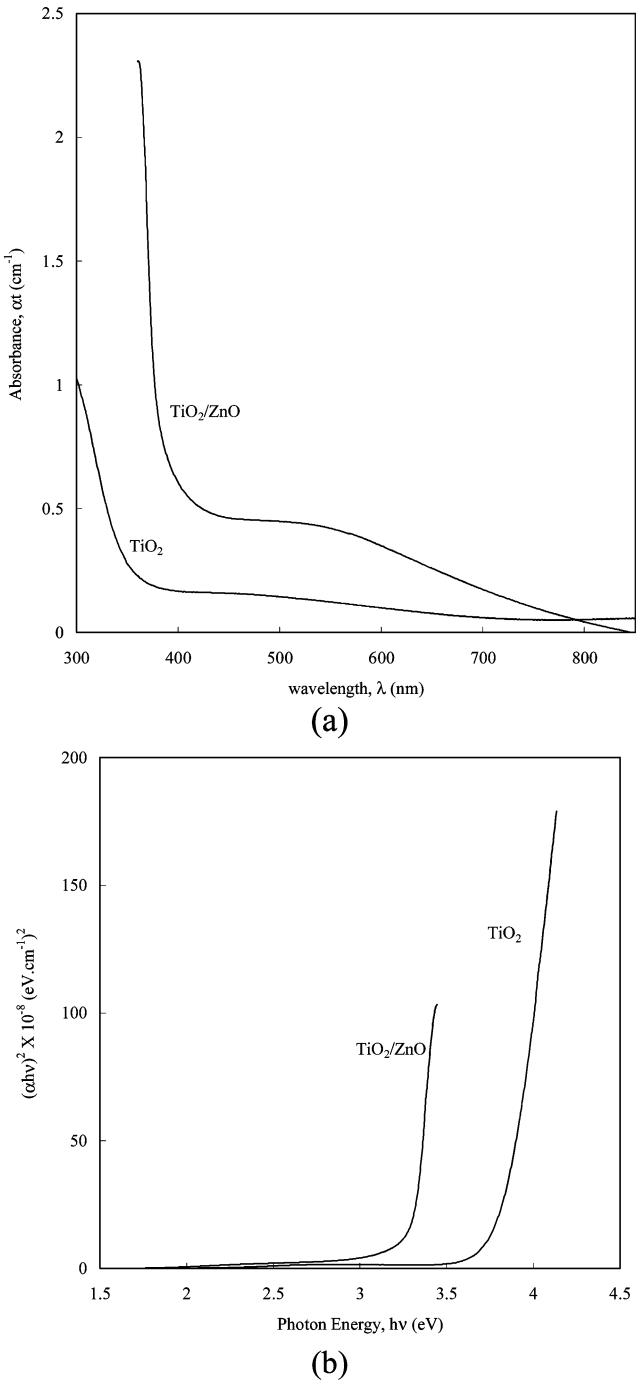

Figure 5. (a) Optical absorption spectrum of a TiO_2 and TiO_2/ZnO film as a function of incident photon energy and (b) measurement of the band gap energy calculated by extrapolating the linear portion to zero absorption coefficient.

angle after ZnO deposition is attributable to (a) the nonspherical nature of the grains and (b) the topographical surface morphology. Because of the conical surface morphology, air trapped in the crevices prevents water from adhering to the film and results in the high water contact angle.

To determine the band gap of the TiO_2 and TiO_2/ZnO films, the spectrum shown in Figure 5a was replotted in the form shown in Figure 5b, using the formula, $\alpha = A/t$. Here, A = absorbance, t = the film thickness (TiO_2 + ZnO = 1.418 μm), α is the absorption (or attenuation) coefficient, and E is the photon energy ($E = h\nu$). The theory of optical absorption provides the relationship between the absorption coefficient and the photon energy, $h\nu$, for direct, allowed transitions as $\alpha = (h\nu - E_g)^{1/2}/h\upsilon$. This allows for calculation of the band gap (E_g) when the linear portion $(\alpha h\nu)^2$ is plotted versus hυ and extrapolated to $\alpha = 0$. Figure 5b shows a plot of $(\alpha h\upsilon)^2$ vs hυ for a TiO_2 and TiO_2/ZnO film. The estimated band gaps of TiO_2 and TiO_2/ZnO were 3.85 and 3.26 eV, repectively. The band gap of TiO_2/ZnO is different to both TiO_2 or ZnO,[24−26] which would be the result of co-deposited TiO_2/ZnO, as reported by Liao et al.[16] for ZnS/ZnO composite thin films. We can infer that the band gap energy is partially dependent on the crystallinity of the film, as the band gap energies of highly crystalline thin films are similar to those of crystalline bulk materials, whereas amorphous or poorly crystallized films show band gap energies higher than those of the corresponding bulk materials. The decrease in the band gap energy is possibly due to the high crystallinity of the ZnO cone-like morphology in the films, and this finding is supported by data from other studies.[18,27]

The conical morphology of the ZnO as seen in the SEM data is useful for application in dye-sensitized TiO_2/ZnO electrodes in solar cells, as after dye adsorption in the ZnO cones, the surface becomes dark red (see earlier). The thin sputtered Pt layer on the ITO glass was used as the counter electrode, and this played the role of a catalyst facilitating the reduction of I_3^- ions and improving the rejuvenation efficiency of the dye. Recently, a fast charge transport using an I^-/I_3^- redox couple in the presence of an ionic liquid electrolyte was observed, due to the contribution of the exchange reaction between I^- and I_3^-. Kawano et al.[28] reported that this contribution to the total charge transport current dominated when the concentration of the redox couple was high and the $[I^-]$ and $[I_3^-]$ were similar. The adsorption of N3 dye into the porous metal oxide[29] was higher than that in a compact,[30] and the presence of the extremely thin TiO_2 nanocrystalline film did not contribute to any dye adsorption.

It is known that ZnO is not excited by visible light. The TiO_2/ZnO film electrodes were kept at 45 °C in N3 dye for 48 h. The power conversion efficiency was calculated from the relationship, $\eta = I_m V_m/p_r \times 100\%$, where $I_m V_m$ is the maximum multiplied value in the I−V sweep, and p_r is the illumination power input, which was controlled to 80 mW/cm^2. The open circuit voltage (V_{oc}) was set at $I = 0$, and the short circuit current was defined at $V = 0$. Figure 6a shows the I−V curves for a TiO_2/ZnO electrode with a *t*-BPy electrolyte added in addition to the normal lithium iodide electrolyte. (The dark circles and open rectangles denote the normal lithium iodide, and the open triangles denote the *t*-BPy modified lithium iodide electrolyte, respectively.) The addition of *t*-BPy to the ionic liquid caused a considerable increase in V_{oc} from 0.27 to 0.35 V, with an increase in I_{sc} from 0.10 to 0.39 mA. This is thought to be due to an inhibition of the back electron transfer from the conduction band of ZnO to the dye cations and/or I_3^- ions and by a rise in the Fermi energy level due to the adsorption of *t*-BPy onto the surface of the ZnO. The change in I_{sc} and V_{oc} upon the addition of the modified electrolyte may therefore be attributable to an inhibition of the back electron transfer and a rise in the Fermi energy level, as is used to explain the behavior of organic electrolyte cells. There was almost no adsorption of the dye on the TiO_2 film, and this was attributable to its compact and densely packed smooth nanostructure (not shown), which prohibited dye insertion. The I−V performance of the dye-sensitized TiO_2/ZnO electrode showed a decrease in the recombination rate, with a 0.67% device power conversion efficiency, due to the presence of the TiO_2 energy barrier layer. In the absence of a compact TiO_2 layer, observed efficiency was low, suggesting a thin TiO_2 compact layer offers a more

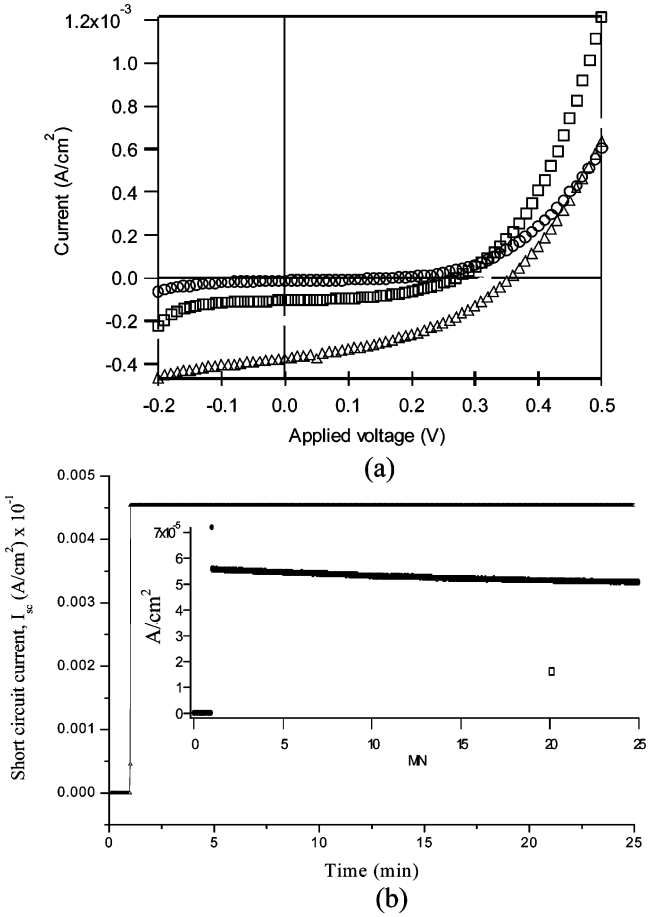

Figure 6. (a) I−V characteristics of a dye-sensitized TiO2/ZnO electrode in the dark (circles), without a *t*-Bpy electrolyte (squares), and with a *t*-BPy electrolyte (triangles). (b) The stability of a dye-sensitized TiO_2/ZnO solar cell with and without (inset) a *t*-BPy electrolyte for 25 min.

seamless electron transport. A similar electron accelerating mechanism is also seen in the post-treatment of $TiCl_4$ in TiO_2-based dye-sensitized solar cells, which facilitates the percolation of electrons from one particle to another.[24] An increase in fill factor (0.47%) in the lithium iodide electrolyte was observed when compared with the fill factor of the modified electrolyte (0.34%), and the change in V_{oc} and I_{sc}, which exhibited an inversely proportional relationship, is attributable to *t*-BPy. However, in the presence of the *t*-BPy electrolyte, a decrease in the series resistance with a relatively high shunt resistance was confirmed (from the large sweep area). This indicates that the charge-transfer resistance decreased when the TiO_2/ZnO/dye and *t*-Bpy-added cell was used, which was evidenced by an increase in its photocurrent. From the lower charge-transfer resistance, a larger electron injection driving force and, consequently, a larger I_{sc} can be obtained. This phenomenon is attributable to a decrease in the recombination rate. The parameters affecting the overall performance of a cell are grain size, porosity, surface area, the amount of dye adsorbed, the electrolyte type, and the process for dye rejuvenation. Dye-sensitized ZnO solar cells show a high conversion efficiency.[31] In these devices, the ZnO deposition process leads to the formation of particulate clusters rather than a film with porous nanoparticles, which may contribute to the insufficient surface area for dye adsorption, as well as to a discontinuous electron transport through the large ZnO conical clusters, resulting in a poor power conversion efficiency. In terms of the device power conversion efficiency, we believe that the different resistances present, such as the electrolyte/ZnO interface, the TiO_2/ZnO interface, and the ITO/TiO_2 interface (including the TiO_2 resistance), do not contribute much to the charge-transfer process. In addition, an increase in ZnO could have a negative effect on cell performance. ZnO has a low electron effective mass of about 0.2 m_e.[27] This indicates that ZnO could affect the electrons injected from the dye, resulting in a poor power conversion efficiency.

Figure 6b shows the stability of a dye-sensitized TiO_2/ZnO photovoltaic cell with, and without (inset), a *t*-BPy electrolyte over a period of 25 min. The dye-sensitized TiO_2/ZnO photoelectrode with a *t*-BPy electrolyte showed a consistent short circuit current, which is not exhibited by a cell without a *t*-BPy electrolyte, suggesting that an ionic liquid electrolyte is important for effective charge transport and to protect the device from drying and thus to provide long-term stability.

Conclusion

In this work, TiO_2/ZnO thin film electrodes for dye-sensitized solar cells were fabricated using a chemical bath deposition technique and the LbL method onto an ITO substrate. The as-deposited TiO_2 films were composed of densely packed super-hydrophilic, nanometer-sized spherical grains, where the ZnO deposited on the TiO_2 film showed less hydrophilic character, with a randomly oriented cone-like surface morphology. The direct transition band gap energy of the TiO_2/ZnO system was found to be 3.2 eV. The use of a compact TiO_2 thin layer facilitated the percolation of electrons by acting as an effective hole-blocking layer (HBL) and avoided direct contact of the dye with the ITO, which was responsible for decreasing the charge-transfer resistance. The as-deposited TiO_2/ZnO electrode was found to be stable for a period of 25 min and had a device power conversion efficiency of 0.67%.

Acknowledgment. R.S.M. wishes to thank Brain Korea 21 for the award of a postdoctoral fellowship. This work was supported by the Korean Science and Engineering Foundation (ABRL R14-2003-014-01001-0).

References and Notes

(1) Rao, C. N. R.; Kulkarni, G. U.; Thomas, P. J.; Edwards, P. P. *Chem.−Eur. J.* **2002**, *8*, 28.
(2) Nanda, J.; Narayan, K. S.; Kuruvilla, B. A.; Murthy, G. L.; Sarma, D. D. *Appl. Phys. Lett.* **1998**, *72*, 1335.
(3) Gratzel, M. *Nature* **2001**, *414*, 228.
(4) Nelson, J. *Phys. Rev., B.* **1999**, *23*, 374.
(5) Kong, X.; Sun, X.; Li, X.; Li, Y. *Mater. Chem. Phys.* **2003**, *82*, 997.
(6) Vayssieres, L.; Keis, K.; Hagfeldt, A.; Lindquist, S. E. *Chem. Mater.* **2001**, *13*, 4386.
(7) Xu, C. X.; Sub, X. W.; Chen, B. J.; Shum, P.; Lu, S.; Hu, X. *J. Appl. Phys.* **2004**, *95*, 661.
(8) Hara, K.; Horiguchi, T.; Kinoshita, T.; Sayama, K.; Hugihara, H.; Arakawa, H. *Sol. Energy Mater. Sol. Cells* **2000**, *64*, 115.
(9) Huang, M. H.; Mao, S.; Feick, H.; Yan, H. Q.; Wu, Y. Y.; Kind, H.; Weber, E.; Russo, R.; Yang, P. D. *Science* **2001**, *292*, 1897.
(10) Wu, J. J.; Liu, S. C. *Adv. Mater.* **2002**, *14*, 215.
(11) Kong, X. H.; Sun, X. M.; Li, Y. D. *Chem. Lett.* **2003**, *32*, 546.
(12) Barbe, C. J.; Arendse, F.; Compte, P.; Jirousek, M.; Lenzmann, F.; Shklover, V.; Gratzel, M. *J. Am. Ceram. Soc.* **1997**, *80*, 3157.
(13) Tennakone, K.; Kottegoda, I. R. M.; De Silva, L. A. A.; Perera, V. P. S. *Semicond. Sci. Technol.* **1999**, *14*, 975.
(14) Bandaranayake, P. K. M.; Jayaweera, P. V. V.; Tennakone, K. *Sol. Energy Mater. Sol. Cells* **2003**, *76*, 57.
(15) Tennakone, K.; Bandara, J.; Bandaranayake, P. K. M.; Kumara, G. R. A. Konno, A. *Jpn. J. Appl. Phys.* **2001**, *40*, L732.
(16) Liao, J.-Y.; Ho, K.-C. *Sol. Energy Mater. Sol. Cells* 2004, in press.
(17) Miyasaka, T.; Kijitori, Y. *J. Electrochem. Soc.* **2004**, *151*, A1767.
(18) Rotzinger, F. P.; Gratzel, M. *Inorg. Chem.* **1987**, *26*, 3704.
(19) (a) Muhlebach, J.; Muller, K.; Schwarzenbach G. *Inorg. Chem.* **1970**, *9*, 2381, (b) Gao, Y.; Masuda, Y.; Peng, Z.; Yonezawa, T.; Koumoto, K. *J. Mater. Chem.* **2003**, *13*, 608.
(20) Zumeta, I.; Esinosa, R.; Ayllon, J. A.; Vigil, E. *Semicond. Sci. Technol.* **2002**, *17*, 1218.

(21) Lokhande, C. D.; Lee, E.-H.; Jung, K. -D.; Joo, O.-S. *J. Mater. Sci.* **2004**, *39*, 2915.

(22) Wang, X.-P.; Yu, Y.; Hu, X.-F.; Gao, L. *Thin Solid Films* **2000**, *371*, 148.

(23) Sun, R.-D.; Nakajima, A.; Fujishima, A.; Watanabe, T.; Hashimoto, K. *J. Phys. Chem. B.* **2001**, *105*, 1984.

(24) Mane, R. S.; Roh, S. J.; Joo, O.-S.; Lokhande, C. D.; Han, S.-H. *Electrochim. Acta* **2005**, *50*, 2453.

(25) (a) Mane, R. S.; Roh, S. J.; Han, S.-H. *Chem. Lett.* **2005**, *34*, 536. (b) Shinde, V. R.; Lokhande, C. D.; Mane, R. S.; Han, S.-H. *Appl. Surf. Sci.* **2005**, *245*, 407.

(26) Lindroos, S.; Leskela, M. *Int. J. Inorg. Mater.* **2000**, *2*, 197.

(27) Ivanova, T.; Harizanova, A.; Surtchev, M. *Mater. Lett.* **2002**, *55*, 327.

(28) Kawano, R.; Matsui, H.; Matsuyama, C.; Sato, A.; Hasan Susan A. B.; Tanabe, N.; Watanabe, M. *J. Photochem. Photobiol., A* **2004**, *164*, 87.

(29) Kosacki, I.; Petrovski, V.; Anderson, H. U. *Appl. Phys. Lett.* **1999**, *74*, 341.

(30) Mane, R. S.; Hwang, S. H.; Lokhande, C. D.; Sartale, S. D.; Han, S.-H. *Appl. Surf. Sci.* **2005**, *246*, 271.

(31) Keis, K.; Magnusson, E.; Linstrom, H.; Lindquist, S. E.; Hagfeldt, A. *Sol. Energy Mater. Sol. Cells* **2002**, *73*, 51.